

Propagation of Muons Underground and the Primary Cosmic-Ray Spectrum Below 40 TeV

Keran O'Brien

Health and Safety Laboratory, U. S. Atomic Energy Commission, New York, New York 10014
(Received 28 May 1971)

The vertical muon attenuation curve deep underground has been analyzed through the medium of a nucleonic cascade model, to yield a primary cosmic-ray nucleon spectrum in the energy region below 40 TeV. Calculations of the angular distribution of muons underground reproduce the Utah experimental results within about 20% without the need to postulate the X process. At these energies it is concluded that the hadron absorption cross section is, to good approximation, constant and geometric, and that the partial inelasticities are also constant.

I. INTRODUCTION

Muons are the most penetrating of the readily detectable cosmic rays, and fluxes have been measured down to a depth of 9×10^5 g/cm² below the earth's surface (9000 m of water equivalent). The resulting absorption curve underground can be analyzed to yield both the sea-level muon spectrum and the primary cosmic-ray nucleon spectrum.¹

In this report, an assumed trial primary nucleon spectrum is used in combination with an extranuclear cascade transport code² to generate secondary pions throughout the atmosphere. The muons resulting from pion decay are absorbed in the earth and the resulting absorption curve is compared with the experimental curve. Any discrepancies between the theoretical curve and the measured curve can be removed by adjusting the primary nucleon spectrum and recalculating.

Using the primary nucleon spectrum obtained in this way, angular muon distributions were calculated and compared to the angular distributions obtained in the Utah mines. Agreement to within 20% on an absolute basis was found without postulating the X process or other unconventional processes.

II. THE NUCLEONIC CASCADE

An analytical solution to the Boltzmann equation for hadron transport with constant geometric cross sections and constant partial inelasticities has been developed and applied to the case of accelerator beams.² Agreement with experiment and with Monte Carlo calculations of the same quantities was extremely good in the range from 1 to 18 GeV.^{2,3}

Calculations of the propagation of atmospheric

cosmic rays have also been carried out on the same basis.^{4,5} In those calculations, and in the ones described here, the atmosphere is represented as a flat isothermal slab with a scale height of 6.7 km. The cascade is treated as purely nucleonic (see Fig. 1 of O'Brien⁴), and the resulting pions are either absorbed or decay to muons. Muons from kaon decay make only a small contribution to the flux and will be neglected here.⁴ The partial inelasticities used in the calculation are taken from Ref. 5 and are given in Table I.

Secondary hadron production was calculated using the "power-law" model⁵ which is devised so as to agree with the partial inelasticities of Table I and the secondary particle multiplicities of Meyer *et al.*⁶

III. MUON TRANSPORT

A. Muon Stopping Power

Muons lose energy by four processes: ionization, pair production, bremsstrahlung, and nuclear interactions. The ionization loss is given by

$$S_i(E) = \frac{0.3072}{\beta^2} \frac{Z}{A} \left[\ln \left(\frac{1.022 \times 10^6}{I} \eta^2 \right) - \beta^2 - \frac{\delta}{2} \right], \quad (1)$$

where $S_i(E)$ is the energy loss due to ionization in MeV cm²/g, evaluated at energy E , β is the muon velocity relative to the speed of light, η is the ratio of muon momentum to muon rest mass ($= pc/m_\mu c^2$), I is the ionization potential of the medium in eV, Z and A are the conventional symbols for atomic number and weight, and δ is the density effect. Armstrong and Alsmiller give for the density effect⁷

$$\delta = \ln \left(8.306 \times 10^2 \frac{Z}{A} \eta^2 \frac{\rho}{F^2} \right), \quad (1a)$$

TABLE I. Partial inelasticities for nucleon-air collisions.

q	K_q
p	0.211
n	0.211
π^\pm	0.292
π^0	0.180
K	0.090

where ρ is the density of the material in g/cm^3 . When δ takes on negative values, it is to be replaced by zero.

The energy loss due to bremsstrahlung and pair production is given by

$$S_b(E) = b_b(Z^2/A)E, \quad (2)$$

$$S_{pp}(E) = b_{pp}(Z^2/A)E,$$

where E is the muon kinetic energy in MeV, b_b is the energy-loss coefficient for bremsstrahlung, and b_{pp} is the energy-loss coefficient for pair production. Recent calculations^{8,9} suggest a value of a little over 4×10^{-7} for b_{pp} and a value of just over 3×10^{-7} for b_b .⁸ This is in agreement for the value calculated by Meyer *et al.*¹⁰ for the sum of the two processes, which is adopted, giving

$$S_{b+pp}(E) = 7.34 \times 10^{-7}(Z^2/A)E. \quad (3)$$

The energy loss due to photonuclear interactions is given by

$$S_{pn}(E) = 4.26 \times 10^{21} \sigma_{hv} E, \quad (4)$$

where σ_{hv} is the photonuclear cross section.

Meyer *et al.*¹⁰ have shown that the theoretical and experimental muon attenuation curves at great depths can be made to agree if $\sigma_{hv} = 250 \mu\text{b/nucleon}$ on the assumption that the sea-level muon spectral

TABLE II. Properties of air and standard rock.

	A	Z	I (eV)	Density (g/cm^3)
Air	14.485	7.22	93	x/H^a
Standard rock	22	11	124	2.65

^aAir density is a function of atmospheric depth, and in an isothermal atmosphere is proportional to the inverse scale height. Here $H = 6.7 \times 10^5$ cm, and x is atmospheric depth in g/cm^2 .

index is 2.6. Adopting this value, the total stopping power is

$$S(E) = \frac{0.3072}{\beta^2} \frac{Z}{A} \left[\ln \left(\frac{1.022 \times 10^6}{I} \eta^2 \right) - \beta^2 - \frac{\delta}{2} \right] + \left(7.34 \times 10^{-7} \frac{Z^2}{A} + 1.06 \times 10^{-6} \right) E. \quad (5)$$

In the calculations to follow, the earth is assumed to be composed, as is customary, of "standard rock." The properties of air and standard rock are shown in Table II.

B. Muon Straggling

Given the sea-level muon spectrum, $\varphi_\mu(E_B, 0)$, per cm^2 per second per steradian in the vertical direction as a function of kinetic energy E_B , the muon spectrum in the same units at a depth r in standard rock in the continuous-slowing-down, straight-ahead approximation is given by¹¹

$$\varphi_\mu(E, r) = \varphi_\mu(E_B, 0) \frac{S(E_B)}{S(E)} \exp \left(- \int_E^{E_B} \frac{dE'}{\lambda(E') S(E')} \right), \quad (6)$$

where E is the energy the muon has at a depth r ,

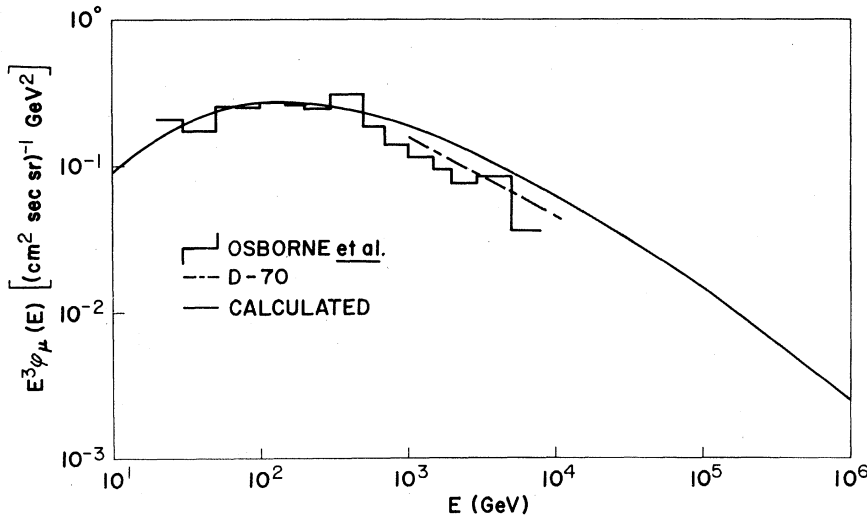


FIG. 1. Comparison of the vertical sea-level muon spectrum calculated in this study with the muon spectra of Osborne *et al.* (Ref. 14) and of Király and Wolfendale (D-70) (Ref. 1).

starting from its initial energy E_B , $S(E)$ is the stopping power in standard rock evaluated at an energy E , and $\lambda(E)$ is the mean free path for muon decay per g/cm^2 .

The relationship between E , E_B , and r is given formally by

$$r = \int_E^{E_B} \frac{dE'}{S(E')} \quad (6a)$$

and the decay probability is obtained from

$$\lambda(E) = \left(\frac{pc}{m_\mu c^2} \right) c\tau\rho, \quad (6b)$$

where p is the muon momentum, c is the velocity of light *in vacuo*, τ is the rest-frame muon lifetime ($= 2.2 \mu\text{sec}$), and ρ is the density of standard rock. The stopping power is written as

$$S(E) = S_i(E) + 5.1 \times 10^{-6}E. \quad (6c)$$

Equations (6) assume that slowing down is continuous. However, the bremsstrahlung and photo-nuclear processes involve large energy transfers, and underground muon fluxes calculated by Eqs. (6) will be too large. This effect amounts to only about a factor of 2 in 1 Mg/cm^2 (1 $\text{Mg}/\text{cm}^2 = 10^6 \text{g}/\text{cm}^2 = 10^4 \text{m}$ of water equivalent). By comparison, the sea-level muon flux has been attenuated by about 9 orders of magnitude. This is the sort of change in intensity that would be brought about by a small reduction in the stopping power, and suggests that the effect of fluctuations on muon penetration to great depths can be accounted for by using a modified stopping power. Accordingly, introduce

$$S^f(E) = S_i(E) + FbE, \quad (7)$$

where F is chosen so that when $S^f(E)$ replaces $S(E)$ in Eqs. (6) the correct flux is obtained.

Kobayakawa¹² has calculated the ratio

$$R(r) = \frac{\int_0^\infty dE \varphi_\mu^f(E, r)}{\int_0^\infty dE \varphi_\mu(E, r)}, \quad (8)$$

where $\varphi_\mu^f(E, r)$ is the muon flux with straggling taken into account, for sea-level muon spectra of the form

$$\varphi_\mu(E_B, 0) \propto E_B^{-\gamma-1}.$$

He shows that $\gamma = 2.5$ well represents the underground attenuation data, and that the ratio $R(r)$ is insensitive to the parameters of the calculation.

Kobayakawa's work is applied to this study by choosing a value of F which, when $\gamma = 2.5$, gives values of $R(r)$ which agree with his results. By this means F is determined to be 0.9275. The precise ratios obtained are shown in Table III. The largest discrepancy with Kobayakawa's results in this representation is 6%.

IV. THE TRIAL PRIMARY SPECTRUM

The vertical pion, nucleon, and muon spectra at sea level were calculated in the energy range 1–1000 GeV by means of the theory discussed in Sec. III.⁵ Agreement using the primary spectrum proposed by Peters¹³ was excellent. The integral nucleon flux per cm^2 per second per steradian is obtained from

$$\log_{10} \varphi(>E) = \alpha - 0.0495[11.9 + \log_{10}(1.7 + E)]^2, \quad (9)$$

where $\varphi(>E)$ is the integral flux of nucleons with energy greater than E , E is the nucleon energy in GeV, and α is 6.885.

For the transport calculations the differential form is required, this is obtained by differentiating Eq. (9),

$$\begin{aligned} \log_{10} \varphi(E) = & (\alpha - 3) - 0.0495[11.9 + \log_{10}(1.7 + E)]^2 \\ & + \log_{10} \{0.099[11.9 + \log_{10}(1.7 + E)] / (1.7 + E)\}, \end{aligned} \quad (10)$$

where $\varphi(E)$ is the differential nucleon flux per ($\text{cm}^2 \text{sec MeV sr}$) at E GeV. When the total particle spectrum is wanted, $\alpha = 7.03$, and when the proton spectrum is wanted, $\alpha = 6.73$.

TABLE III. Comparison of the ratio of the cosmic-ray muon flux calculated neglecting straggling, and including its effect as obtained in this study and as obtained by Kobayakawa (Ref. 12).

Depth (Mg/cm^2)	Present study ($F = 0.9275$)	Kobayakawa	% Difference [(K - Ps)/K] $\times 100$
0.4	0.85	0.84	1.2
0.6	0.66	0.70	5.7
0.8	0.53	0.55	3.6
1.0	0.43	0.43	0.0

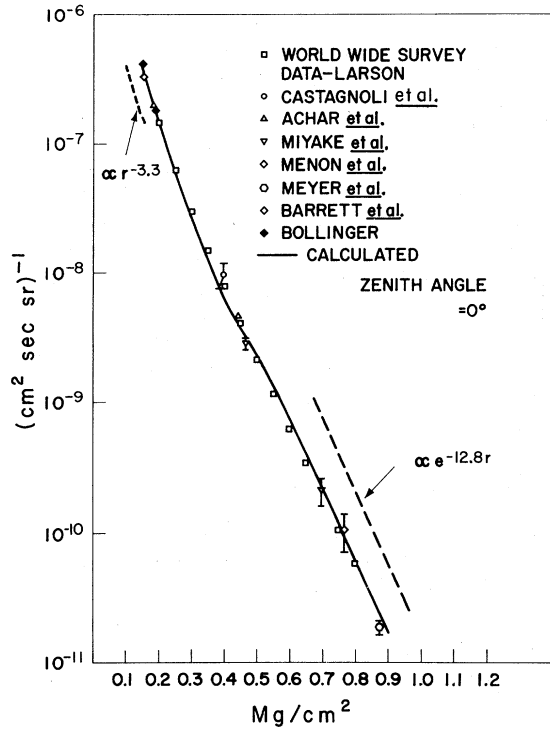


FIG. 2. Comparison of the vertical muon attenuation curve underground calculated in this study, using the primary cosmic-ray nucleon spectrum of Peters (Ref. 13), with experimental data (Refs. 10 and 15-20) and the world-wide survey data of Larson (Ref. 21).

V. CALCULATED MUON FLUXES UNDERGROUND

A. The Incident Muon Spectrum

The trial primary spectrum yields a muon spectrum at sea level as shown in Fig. 1. The two

spectra obtained by Osborne *et al.*¹⁴ and by Király and Wolfendale¹ (known as *D-70*) are shown for comparison. At energies below 1 TeV agreement with the Osborne *et al.*¹⁴ spectrum is very close as this is based on the same data as the comparison carried out earlier.⁵ Above 1 TeV both the Osborne *et al.* spectrum and *D-70* depend on an analysis of underground muon fluxes, the main difference being that the later curve for *D-70* assumes a larger value for the stopping power. Referring to Eq. (6c), the high-energy part of Osborne *et al.* was derived on the basis of

$$S(E) = a + bE,$$

with *b* a constant having a value of 4.0×10^{-6} [here, as in Eq. (6c), *E* is in MeV], whereas the later spectrum was derived on the basis that *b* had the value 4.1×10^{-6} at 1 TeV and 4.3×10^{-6} at 10 TeV. The results of both Osborne *et al.* and *D-70* lie below the calculated muon flux. Had the value for *b* of 5.1×10^{-6} suggested by Meyer *et al.*¹⁰ been used by these authors, the difference between the spectrum calculated for the present study (by the methods of Ref. 5), which at high energies has almost no dependence on the form of the stopping power, and the spectra derived from the underground data, which are very sensitive to it, would be quite small. As it is, the ratio between the calculated spectrum and *D-70* at 10^4 GeV is 1.4 to 1.

B. The Vertical Muon Attenuation Curve

The calculated and measured vertical muon attenuation curve is shown in Fig. 2. Agreement with experimental data is quite good^{10,15-20} over the whole range of depths, indicating that the trial

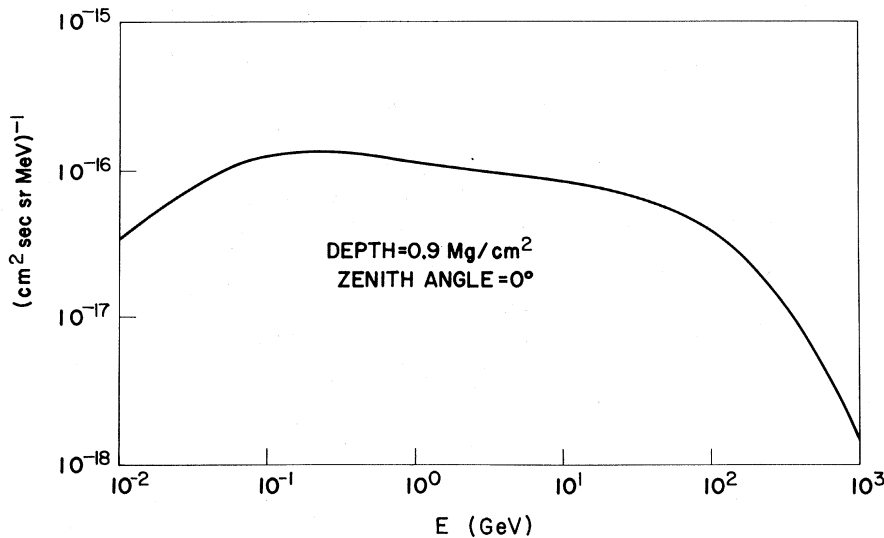


FIG. 3. Calculated vertical muon spectrum at a depth of 9×10^5 g/cm² of standard rock.

spectrum is essentially correct up to the highest energies considered. It is convenient to include the fit to the world survey of muon data made by Larson,²¹ since these points are the basis for the Utah anomaly, to be discussed later. It should be noted that the points from this fit shown in Fig. 2 are not independent of the other data.

To determine the primary spectral energy which controls the muon intensity at a given depth, it is necessary to know the shape of the underground muon spectrum. The calculated muon spectrum at 0.9 Mg/cm² is shown in Fig. 3. Spectra at other depths and zenith angles differ somewhat in their flatness and the rate of "roll-off" above 100 GeV, but all are qualitatively similar in shape and in that 50% of the muons lie in the range 0.1 to 100 GeV. This range of energies is adopted to provide an indication of the dependence of the response of underground muon detectors on the sea-level muon and primary nucleon spectra. We perform the integration [Eq. (6a)]

TABLE IV. Energy interval of the sea-level muon spectrum that governs the muon flux at a given depth underground.

Depth (Mg/cm ²)	Muon spectrum	
	Lower limit (GeV)	Upper limit (GeV)
0.10	2.41 × 10 ²	4.01 × 10 ²
0.15	4.11 × 10 ²	6.14 × 10 ²
0.20	6.26 × 10 ²	8.84 × 10 ²
0.25	9.00 × 10 ²	1.23 × 10 ³
0.30	1.25 × 10 ³	1.66 × 10 ³
0.35	1.68 × 10 ³	2.21 × 10 ³
0.40	2.24 × 10 ³	2.90 × 10 ³
0.45	2.94 × 10 ³	3.78 × 10 ³
0.50	3.83 × 10 ³	4.90 × 10 ³
0.55	4.96 × 10 ³	6.31 × 10 ³
0.60	6.39 × 10 ³	8.10 × 10 ³
0.65	8.21 × 10 ³	1.04 × 10 ⁴
0.70	1.05 × 10 ⁴	1.32 × 10 ⁴
0.75	1.34 × 10 ⁴	1.69 × 10 ⁴
0.80	1.71 × 10 ⁴	2.15 × 10 ⁴
0.85	2.18 × 10 ⁴	2.73 × 10 ⁴
0.90	2.77 × 10 ⁴	3.47 × 10 ⁴
0.95	3.52 × 10 ⁴	4.41 × 10 ⁴
1.00	4.47 × 10 ⁴	5.60 × 10 ⁴

$$r = \int_E^{E_B} \frac{dE'}{S^f(E')}$$

for a fixed r ; with $E = 100$ MeV we obtain the lower limit and with $E = 100$ GeV the upper limit of the energy interval of the spectrum of the sea-level muons that slow down into that region. The results of this calculation are shown in Table IV. The corresponding energy range of the primary nucleon spectrum is gotten by noting that the relation between a muon produced through pion decay and the initiating pion is

$$E_\mu + (m_\mu/m_\pi)E_\pi = 0.76 E_\pi \quad (11)$$

and that

$$\varphi_\pi(E) \cong \frac{\int_E^\infty \varphi(E') F_{\pi\pi} \sigma dE'}{\left(\sigma + \frac{m_\pi c^2}{\tau_\pi c} \frac{H}{x} \frac{1}{p_\pi c}\right)}, \quad (12)$$

where $\varphi(E')$ is the primary differential cosmic-ray nucleon flux, $F_{\pi\pi}$ is the number of pions produced at an energy E' , σ is the (geometric) reaction cross section, τ_π is the rest-frame decay time of the charged pion (= 26.02 nsec), H is the scale height (= 6.7×10^5 cm), and x is the atmospheric depth of pion formation (= 100 g/cm²).²² Noting that σ is constant and representing $F_{\pi\pi}$ by the power-law model,⁵ then, at high energies,

$$\varphi_\pi(E) \propto \varphi(E) \quad (13)$$

and the muon energy intervals can be converted by Eq. (11) to the corresponding intervals of the nucleon spectrum. These intervals correspond to an approximate threshold, the lowest energies of the primary cosmic-ray nucleon spectrum which can produce the muon fluxes at a depth r to which the muon detectors principally will respond, as the integral of Eq. (12) indicates. On this basis [i.e., Table IV and Eq. (11)] it can be seen that the deepest point, of Meyer *et al.*,¹⁰ corresponds to about 3.6×10^4 GeV in the primary spectrum and about 2.7×10^4 GeV in the sea-level muon spectrum.

A knee exists in the attenuation curve at 0.5 Mg/cm², dividing it into two regions with different behavior. This can be explained as follows. First, approximate the vertical sea-level muon flux by

$$\varphi_\mu(E_B, 0) = A E_B^{-\gamma-1}. \quad (14)$$

At low energies, $\gamma = 2.3$ (see Fig. 1), and the stopping power [Eq. (7)] is

$$S^f(E) = \sim 1.88. \quad (15)$$

Substituting Eqs. (14) and (15) into Eq. (6) gives

$$\varphi_\mu(r) \propto r^{-3.3}. \quad (16)$$

At high energies

$$S^f(E) = FbE \quad (17)$$

and $\gamma=2.7$ (Fig. 1 again). This results in

$$\varphi_\mu \propto \exp(-F\gamma br) = \exp(-12.8r). \quad (18)$$

Meyer *et al.*¹⁰ have carried out a least-squares analysis of the vertical muon data at depths greater than 0.4 Mg/cm² of standard rock, fitting them to

$$\varphi_\mu \propto \exp(-r/\lambda). \quad (19)$$

They obtained $\lambda = 0.0804_{-0.0039}^{+0.0035}$ Mg/cm². Comparing Eqs. (18) and (19) it is seen that $\lambda = 1/F\gamma b = 0.0781$, which is excellent agreement. This is also indicated in Fig. 2. The knee in the curve occurs in the region of the transition between the part of the absorption curve governed by Eq. (16) and the part governed by Eq. (18).

C. The Primary Spectrum

The trial spectrum in Eqs. (9) and (10) is based on geomagnetic data at low energies, the emulsion data of Kaplon *et al.*²³ and Barrett *et al.*,¹⁹ and the Linsley air-shower data at high energies.²⁴ This spectrum, Eq. (9), is shown in Fig. 4 along with other emulsion measurements,^{25,26} two extensive air-shower (EAS) measurements,^{27,28} and two satellite measurements.^{29,30}

The spectrum inferred by Brooke *et al.*³¹ from sea-level nucleon measurements has not been included, as it has been shown that the sea-level spectrum can be obtained from the trial spectrum, Eq. (10).⁵

It is noted at this point that the primary spectrum below 10⁶ GeV is assumed to be 91.5% protons, 6.5% α particles, and 1% heavier nuclei,¹³

so that EAS measurements of the integral particle spectrum are multiplied by 0.7 and measurements of the proton spectrum are multiplied by 10/7 to reduce them to the same footing, which in this case is the nucleon spectrum.

Finally, the results of Király and Wolfendale¹ are included. This spectrum, like the one in Fig. 1 on which it is based, is marked D-70.

The trial primary spectrum agrees with most of the emulsion data (except McCusker and Peak²⁶), and is consistent with the Bolivian Air Shower Joint Experiment (BASJE) data reported by La Pointe *et al.*²⁷ In addition, while it lies above D-70, the difference may be due to the nuclear model assumed in going from the muon data of Fig. 1 to the nucleon data of Fig. 4, since the muon spectra of Fig. 1 are considerably closer together.

The trial primary spectrum yields an attenuation curve in excellent agreement with measurement as has been noted above and shown in Fig. 2. The last point, however, corresponding to about 3.6×10^4 GeV in Fig. 4, is 2 standard deviations below the calculated line (~30%), and suggests that the trial spectrum is somewhat too high starting somewhere around 2×10^4 GeV. If this were so, it would agree more closely with D-70 and with the BASJE data than it appears to now. It is felt that further measurements deeper than 0.8 Mg/cm² would be required to settle the point.

The behavior of the satellite data remains an unsolved problem. Grigorov *et al.*³⁰ have attempted to show that the "Proton" satellite data are consistent with the atmospheric nucleonic fluxes if an energy-dependent cross section for nucleon absorption is used. This possibility cannot be ruled out, out of hand, but it does not appear likely as

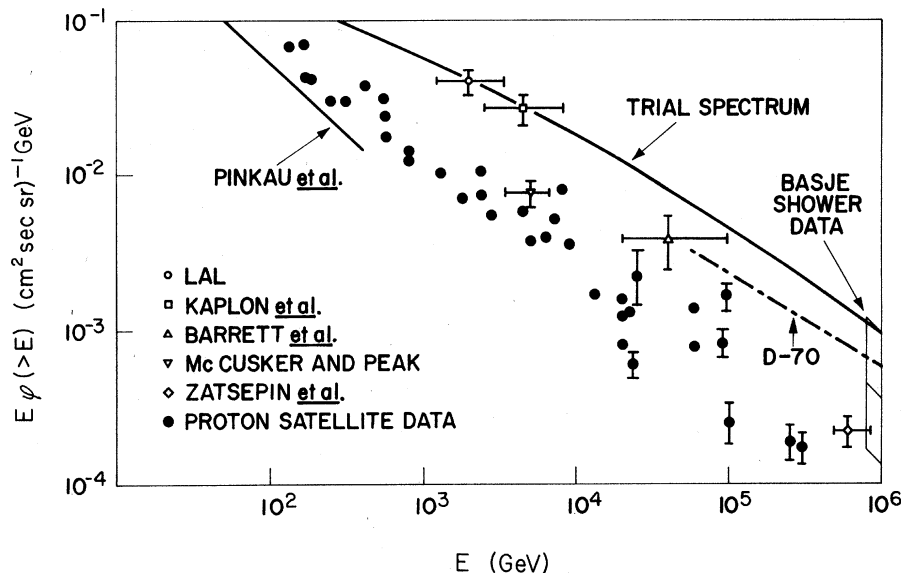


FIG. 4. The primary cosmic-ray integral nucleon spectrum inferred from various measurements (Refs. 19, 23, and 25-30) and the trial cosmic-ray nucleon spectrum used in this study.

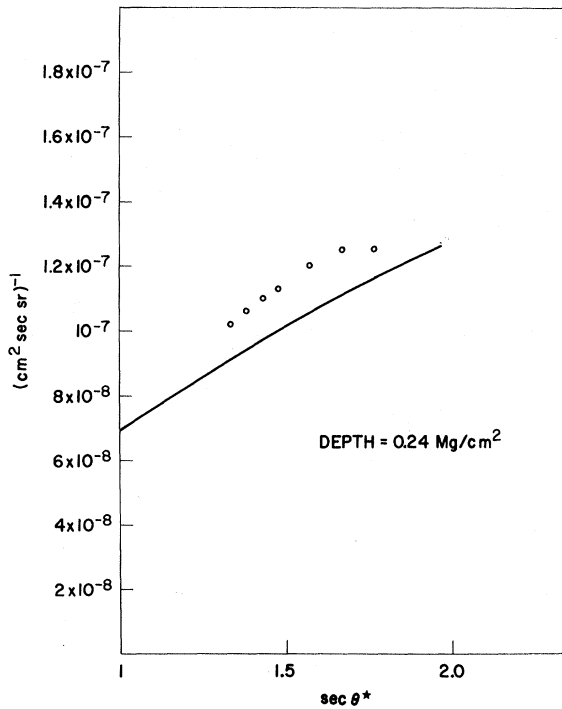


FIG. 5. Cosmic-ray muon flux at a depth of 2.4×10^5 g/cm² as a function of the secant of the zenith angle θ^* calculated in this study and measured by Bergeson *et al.* (Ref. 34).

both the nucleon spectrum up to 4 TeV (Ref. 5) and the muon spectrum up to 10 TeV in this paper have been calculated with the trial spectrum and constant cross sections, and have yielded good results. The sea-level nucleon spectrum and the sea-level muon spectrum depend quite differently on the nucleon absorption cross section used and it is difficult to see how both spectra can be correctly calculated unless both the incident cosmic-ray spectrum and the cross sections are essentially correct.

To recapitulate, the nucleon spectrum adopted here, Eqs. (9) and (10), is in agreement with the earlier emulsion measurements of the primary cosmic-ray spectrum, and consistent with the BASJE air-shower measurements, though strongly disagreeing with the "Proton" satellite data and with the satellite data of Pinkau *et al.* In addition, there is some evidence from the underground muon measurement of Meyer *et al.*¹⁰ that the trial spectrum is too high above about 20 TeV, which would lead to better agreement with *D-70* and Barrett *et al.*¹⁹ The nucleon spectrum adopted here yields good agreement with the sea-level muon spectrum up to 10 TeV, the sea-level nucleon spectrum up to 4 TeV (Ref. 5), and the vertical muon attenuation curve down to a depth of 0.87 Mg/cm², correspond-

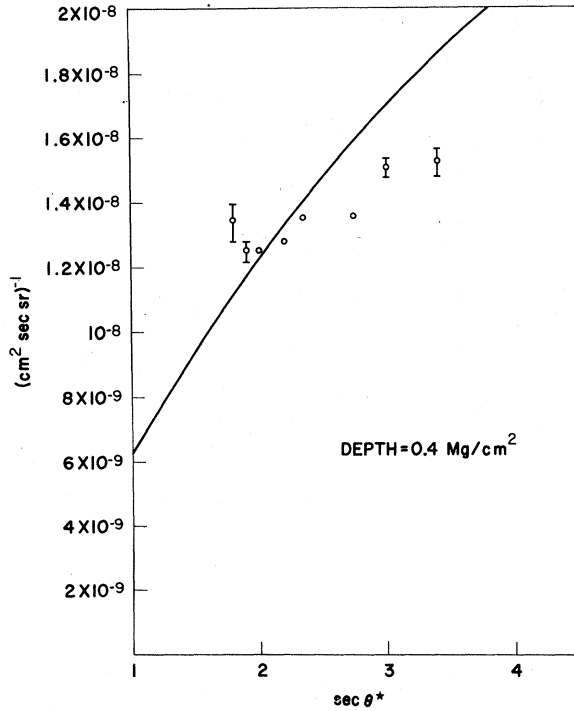


FIG. 6. Cosmic-ray muon flux at a depth of 4×10^5 g/cm² as a function of the secant of the zenith angle θ^* calculated in this study and measured by Bergeson *et al.* (Ref. 34).

ing to a primary nucleon energy of about 36 TeV.

D. The Utah Measurements

Bergeson *et al.*³²⁻³⁴ have proposed the existence of a process, the *X* process, that operates between 1 and 4 TeV, in order to explain the measured angular distributions obtained in the Utah mines. Certainly Eqs. (18) and (19) indicate that the vertical underground muon fluxes at greater depths than 0.5 or 0.6 Mg/cm² (primary nucleon energies 5 or 10 TeV) are inconsistent with the *X* process, in agreement with the observation of Bergeson *et al.* for these energies. However, 1-4-TeV muons correspond to a depth range 0.25 to 0.5 Mg/cm² which is the transition region between "low-energy" slowing down, as described approximately by Eq. (16), and "high-energy" "catastrophic" slowing down described by Eq. (18), so that qualitative arguments based on the vertical flux alone are insufficient.

In Figs. 5-7 angular muon fluxes underground are calculated by means of Eqs. (6) and (7) and compared with the Utah results.³⁴ The first and the last of these were chosen to lie outside the range of the *X* process and the middle graph was chosen to correspond with the depth where the ef-

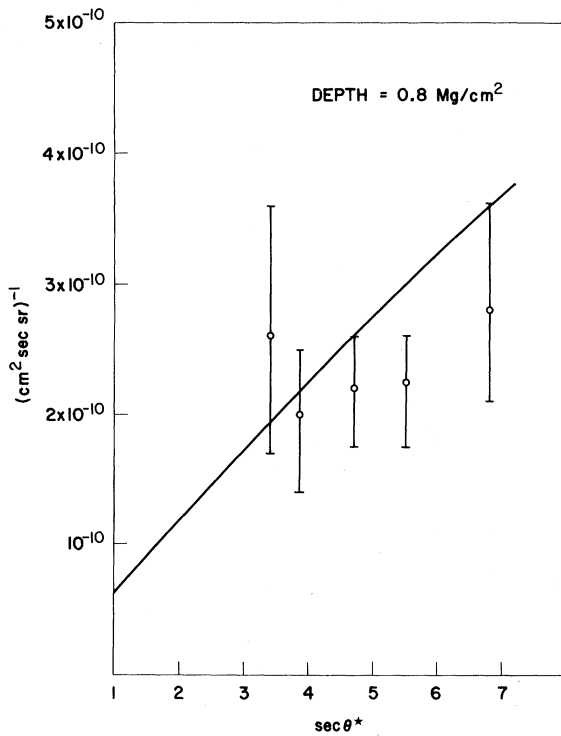


FIG. 7. Cosmic-ray muon flux at a depth of $8 \times 10^5 \text{ g/cm}^2$ as a function of the secant of the zenith angle θ^* calculated in this study and measured by Bergeson *et al.* (Ref. 34).

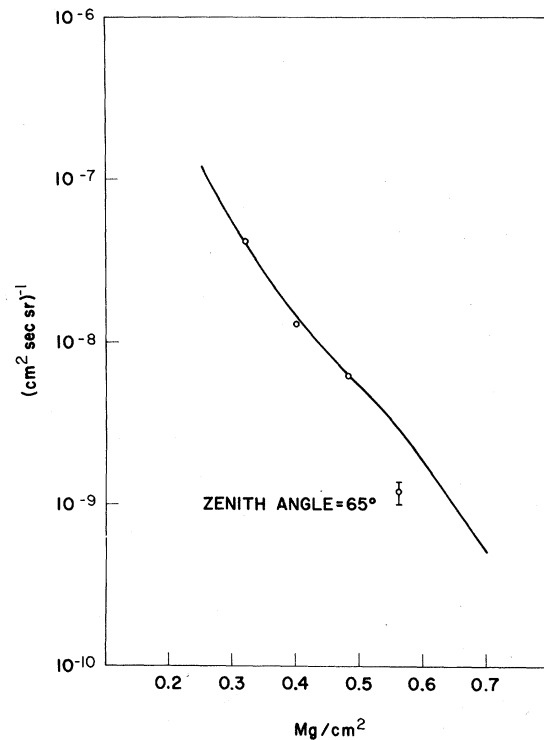


FIG. 8. Comparison of the muon attenuation curve underground at a zenith angle of 65° calculated in this study with the measurements of Bergeson *et al.* (Ref. 34).

fect is expected to be maximum.

Typically, calculation and measurement are within 20%, but the discrepancy is frequently larger than would be predicted on the basis of the size of the statistical errors alone and the experimental values seem to have a different shape than the experimental curve. The world survey data of Larson²¹ to which allusion has already been made, and which anchor the Utah data at 0° , are in agreement with the calculated 0° data as has already been shown (Fig. 2).

In Figs. 8 and 9 attenuation curves for fixed zenith angles of 65° and 75° are shown. Here experimental and theoretical curves have the same shape. The agreement between theory and calculation is excellent in Fig. 8. In Fig. 9, the discrepancy is independent of depth and hence of energy, and thus cannot be due to the X process. The X process would cause the experimental data to deviate downwards near 0.4 Mg/cm^2 in both cases.

VI. CONCLUSIONS

Calculations of cosmic-ray propagation in the atmosphere and underground have been carried out making the following assumptions:

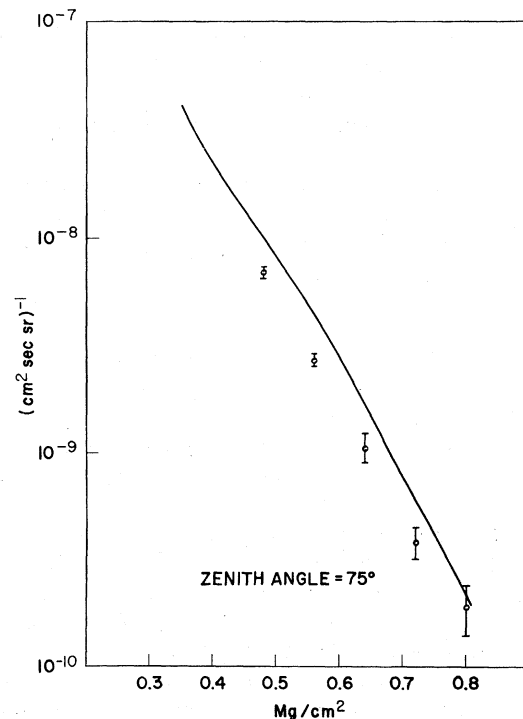


FIG. 9. Comparison of the muon attenuation curve underground at a zenith angle of 75° calculated in this study with the measurements of Bergeson *et al.* (Ref. 34).

(1) The hadron-nucleus absorption cross section is constant, and geometric (at least out to 50 TeV).

(2) The muon photonuclear cross section is 250 μb per nucleon.

(3) The multiplicity of shower particles is the same as that given by Meyer *et al.*⁶

(4) The partial inelasticities (see Table I) are the same as Ref. 5.

(5) There is no X process.

It was concluded that the primary integral nucleon spectrum is given by

$$\log_{10}[\varphi(>E)] = 6.885 - 0.0495[11.9 + \log_{10}(1.7 + E)]^2,$$

$$E < 4 \times 10^4 \text{ GeV},$$

where E is in GeV, and $\varphi(>E)$ is in $(\text{cm}^2 \text{ sec sr})^{-1}$, plus the five assumptions given above, because this spectrum reproduces the vertical muon attenuation curve down to a depth of 0.87 Mg/cm^2 and the angular muon spectra of the Utah group³⁴ to within about 20%, the vertical sea-level muon spectrum up to 10 TeV, and the vertical nucleon spectrum up to 4 TeV.⁵ It has been indicated that there is some evidence that the muon absorption curve underground may be in somewhat better agreement with a primary nucleon spectrum a little lower than that given above 20 TeV.

¹P. Király and A. W. Wolfendale, *Phys. Letters* **32B**, 510 (1970).

²K. O'Brien, *Nucl. Instr. Methods* **72**, 93 (1969).

³T. W. Armstrong and R. G. Alsmiller, Jr., Oak Ridge National Laboratory Report No. ORNL-RSIC-25, ANS-SD-9, 1970 (unpublished).

⁴K. O'Brien, *J. Geophys. Res.* **75**, 4357 (1970).

⁵K. O'Brien, *Nuovo Cimento* **3A**, 521 (1971).

⁶H. Meyer, M. W. Teucher, and E. Lohrmann, *Nuovo Cimento* **28**, 1399 (1963).

⁷T. W. Armstrong and R. G. Alsmiller, Jr., *Nucl. Instr. Methods* **82**, 289 (1970).

⁸A. D. Erlykin, *Acad. Sci. USSR, Physical Series* **29**, 1055-2136 (1965).

⁹S. R. Kel'ner and Yu. D. Kotov, *Yadern. Fiz.* **9**, 1210 (1969) [*Soviet J. Nucl. Phys.* **9**, 708 (1969)].

¹⁰B. S. Meyer, J. P. F. Sellschop, M. F. Crouch, W. R. Kropp, H. W. Sobel, H. S. Gurr, J. Lathrop, and F. Reines, *Phys. Rev. D* **1**, 2229 (1970).

¹¹R. G. Alsmiller, Jr., F. S. Alsmiller, and J. E. Murphy, Oak Ridge National Laboratory Report No. ORNL-3289, 1963 (unpublished).

¹²K. Kobayakawa, *Can. J. Phys.* **46**, S395 (1968).

¹³B. Peters, in *Handbook of Physics*, edited by E. U. Condon and H. Odishaw (McGraw-Hill, New York, 1958), p. 9-207.

¹⁴J. L. Osborne, A. W. Wolfendale, and N. S. Palmer, *Proc. Phys. Soc. (London)* **84**, 911 (1964).

¹⁵C. Castagnoli, A. DeMarco, A. Longhetto, and P. Penengo, *Nuovo Cimento* **35**, 969 (1965).

¹⁶C. V. Achar, V. S. Narasimhan, P. V. Ramana Murthy, D. R. Creed, J. L. Osborne, and A. W. Wolfendale, *Proc. Phys. Soc. (London)* **86**, 1305 (1965).

¹⁷S. Miyake, V. S. Narasimhan, and P. V. Ramana Murthy, *Nuovo Cimento* **32**, 1505 (1964).

¹⁸M. G. K. Menon, S. Naranan, V. S. Narasimhan, K. Hinotani, N. Ito, S. Miyake, D. R. Creed, J. L. Osborne, and A. W. Wolfendale, *Can. J. Phys.* **46**, S344 (1968).

¹⁹P. H. Barrett, L. M. Bollinger, G. Cocconi, Y. Eisenberg, and K. Greisen, *Rev. Mod. Phys.* **24**, 133 (1952).

²⁰L. M. Bollinger, Ph.D. thesis, Cornell University, 1951 (unpublished), reported by Barrett *et al.* (Ref. 19).

²¹M. O. Larson, Ph.D. thesis, University of Utah, 1968 (unpublished).

²²Equation (12) is used as the basis of the rationale in relating the energy of the primary nucleon spectrum to the depth in the earth at which a muon flux is measured. The muon fluxes are not calculated this way however. The full description can be found in Ref. 5, but it is noted here that the calculation involves integrating pion production spectra over the entire atmosphere (0-1033 g/cm^2).

²³M. F. Kaplon, D. M. Ritson, and E. P. Woodruff, *Phys. Rev.* **85**, 933 (1952).

²⁴J. Linsley, *Phys. Rev.* **86**, 1050 (1952).

²⁵D. Lal, *Proc. Indian Aca. Sci.* **A38**, 93 (1953).

²⁶C. B. A. McCusker and L. S. Peak, *Nuovo Cimento* **31**, 525 (1964).

²⁷M. La Pointe, K. Kamata, J. Gaebler, I. Escobar, V. Domingo, K. Suga, K. Murakami, Y. Toyada, and S. Shibata, *Can. J. Phys.* **46**, S68 (1968).

²⁸G. T. Zatsepin, S. I. Nikolsky, and G. B. Christiansen, in *Proceedings of the Eighth International Conference on Cosmic Rays, Jaipur, India, 1963* edited by R. R. Daniel *et al.* (Commercial Printing Press, Bombay, India, 1964-1965), Vol. 4, p. 100.

²⁹K. Pinkau, U. Pollvogt, W. K. H. Schmidt, and R. W. Huggett, in *Proceedings of the Eleventh International Conference on Cosmic Rays, Budapest, 1969*, edited by P. Gombás, *Acta. Phys. Acad. Sci. Hung. Suppl.* **1**, 291 (1970).

³⁰N. L. Grigorov, V. E. Nestorov, I. D. Rapoport, I. A. Savenko, and G. A. Skuridin, *Yadern. Fiz.* **11**, 1058 (1970) [*Soviet J. Nucl. Phys.* **11**, 588 (1970)].

³¹G. Brooke, P. S. Hayman, Y. Kamiya, and A. W. Wolfendale, *Proc. Phys. Soc. (London)* **83**, 853 (1964).

³²H. E. Bergeson, J. W. Keuffel, M. O. Larson, E. R. Martin, and G. W. Mason, *Phys. Rev. Letters* **19**, 1487 (1967).

³³H. E. Bergeson, J. W. Keuffel, M. O. Larson, G. W. Mason, and J. L. Osborne, *Phys. Rev. Letters* **21**, 1089 (1968).

³⁴H. E. Bergeson, G. O. Bolingbroke, D. E. Groom, J. W. Keuffel, and J. L. Osborne, report, 1970 (unpublished).